Evidence for Fermi-Shuttle Ionization in Intermediate Velocity $C^+ + Xe$ Collisions

B. Sulik,[1] Cs. Koncz,[1] K. Tőkési,[1,2] A. Orbán,[1] and D. Berényi[1]

[1]*Institute of Nuclear Research (ATOMKI), H-4001 Debrecen, P.O. Box 51, Hungary*
[2]*Institute for Theoretical Physics, Vienna University of Technology, A-1040 Vienna, Austria*

(Received 27 February 2001; published 31 January 2002)

Experimental evidence has been found for consecutive projectile-target-projectile (triple) and projectile-target-projectile-target (quadruple) "ping-pong" scattering of ionized target electrons in single $C^+ + Xe$ collisions at 150 and 233 keV/u impact energies. Distinct signatures of the multiple electron scattering contributions to the high-energy part (300–3400 eV) of the double differential electron spectra have been separated and identified with the help of reference measurements using He^+ projectile ions and different calculations.

DOI: 10.1103/PhysRevLett.88.073201 PACS numbers: 34.50.Fa

In recent years, several laboratories have started to study the emission of fast electrons in ion-atom [1–3] and ion-solid [4–8] collisions. In some cases, distinct signatures of Fermi-shuttle processes have been found in the electron spectra [1,2,8]. Fermi [9] had proposed the mechanism as a possible origin of cosmic rays; specifically, giant magnetic fields, moving against each other in space, can accelerate charged particles to very high energies in long sequences of reflections. It was later shown that this type of "ping-pong" game can also be played with other "paddles," such as the microscopic fields of atoms, molecules, or clusters [10–14], where even a short sequence of scattering events might be of great interest.

Ionization in ion-atom collisions may include a sequence of backscatterings of a liberated electron between the incoming projectile ion (moving with a velocity V) and the target core. The velocity of the electron is increased by approximately $2V$, in every 180° elastic scattering with the incoming projectile, while only the direction of the electronic motion is changed by the target field. This follows directly from the kinematics of small particles (m) elastically scattered by heavy centers (M) with mass ratios $M/m \gg 1$. Here, we introduce the shorthand P and T to denote the electron-projectile and electron-target scatterings, respectively. In this notation, the so-called binary encounter (BE) ionization of the target [15,16] is denoted by P, while the projectile ionization (also known as electron loss [16]) is denoted by T. Longer sequences can be referred to as, for example, P-T-P or T-P-T-P.

Target ionization sequences start with a P process, and may emit electrons up to the velocity $2nV$ in both forward and backward directions relative to the projectile motion. Here, n is the number of encounters with the projectile. For electron loss sequences (starting with T), the corresponding velocity is $(2n + 1)V$. The observation of such hot electrons is of fundamental importance for basic research in collision physics. They are emitted in particular ionization processes, which can be associated with specific three-body states. Moreover, since fast electrons form a long-range secondary radiation, such an acceleration process may be important in ion-matter interactions, and, therefore, relevant in many applications such as cancer therapy, ion track formation, or the modification of material properties [2,7,14].

The first theoretical evidence for the Fermi-shuttle acceleration of electrons was found by Wang *et al.* [12] by applying a quantum mechanical model with zero-range potentials to two-center collisions. Subsequently, both classical [3,13,14] and quantum mechanical calculations [13,17] have been applied to the ping-pong scenario. No attempt has been made for a full theoretical treatment yet, but some properties can be derived from general considerations. For example, the effective area of an "ion paddle" is roughly proportional to the cross section for 180° elastic electron scattering by its core, i.e., to Z^2 for a bare ion [2]. Large Z's are important for both forming and observing longer sequences. The observability of a P-T-P process on the "background" of the first-order P process, e.g., can be characterized by the ratio $\sigma_{P\text{-}T\text{-}P}/\sigma_P \sim Z_{\text{proj}}^2$. It has been widely recognized [2,3,13,14,17–19] that the screened fields of the collision partners may enhance the forward-backward focusing, compared to the Coulomb fields of bare ions.

In collisions of free atomic species, hot electrons were observed as early as 1979 [20]. Fermi-shuttle acceleration was first identified by Suárez *et al.* [1], as the T-P process in H + He collisions. The first observation of the P-T process in gaseous targets was reported by Bechthold *et al.* [2] in collisions with 5.9 MeV/u U^{27+} ions. Larger yields of fast electrons have been observed in ion-solid collisions [4–8] in a wide (keV–GeV) range of impact energies. This can be explained by the high density of atomic centers in solids [7,14,21]. Recently, Fermi-shuttle acceleration was successfully invoked to explain the high-velocity tail of the spectrum of electrons emitted in 45 MeV/u Ni + Au collisions by Lanzano *et al.* [8]. Single collisions, however, are rather rare events in ion-solid experiments. To investigate the mechanism in more detail, it looks most promising to proceed with thin gaseous targets. In such experiments, only double scattering processes have been observed earlier [1,2].

In this Letter, we report strong evidence for the triple scattering process P-T-P and the quadruple process P-T-P-T in single collisions of ions with free atoms. In earlier experiments [3], we observed an enhanced intensity for the P-T process at 180° in 150 keV/u C^+ + Ne, Ar collisions, so we focused our search in this intermediate velocity region. We analyzed the properties of the ionic cores by calculating their dispersion patterns for elastic electron scattering. To increase the length of the sequences, xenon was selected as the target, and the C^+ ion was selected as the projectile. We searched for distinct structures at the mean velocity of the electrons emitted in P^n-T^m ($n - 1 \leq m \leq n$) sequences, where a general $v(\theta)$ formula derived from simple kinematics is as follows:

$$v = \begin{cases} V(\cos\theta + \sqrt{\cos^2\theta + 4m + 4m^2}) & \text{if } m < n \\ 2nV & \text{if } m = n \end{cases}. \quad (1)$$

In the experiments, double differential cross sections for electron emission were measured for energies of 20–3400 eV and for observation angles $\theta = 0°$–$180°$. The experimental method used was the same as in Ref. [3], so only a brief description is given here. In the measurements, performed at ATOMKI, Debrecen, beams of He^+ ions with 233 keV/u, and C^+ ions with 150 and 233 keV/u energies were directed onto the Xe gas jet target. The electron spectra were collected simultaneously in 13 angular channels with a triple-pass electrostatic spectrometer (ESA-21) [22]. For cross sections $\sigma \geq 10^{-23}$ cm^2/eV sr, the absolute experimental uncertainty was less than 40%. This has been estimated from reference data [23] and the reproducibility of the spectra (≤15%). For testing single collision conditions, the effective target density was varied between 10^{12} and 10^{13} atom/cm^3, and no difference between the spectra was found within the statistical uncertainties.

Double differential electron emission cross sections measured for 150 keV/u ($V = 2.45$ a.u.) C^+ + Xe collisions are shown in Fig. 1. Low-energy electron emission is dominated by target ionization, while the electron loss (EL) peak (T process) appears at the so-called cusp energy, 81.8 eV. The carbon K-Auger group originating from the moving projectile is shifted in energy with the observation angle as expected. Xenon-Auger contributions have been found to be negligible in the energy region of interest. The energy position of the BE peak follows from Eq. (1) (with $n = 1$, $m = 0$), forming the single scattering binary ridge, indicated by the P curve. The double scattering P-T ridge ($n = 1$, $m = 1$) at the constant energy of 328 eV is clearly observable at backward angles. The next acceleration phase ($n = 2$, $m = 1$) forms the P-T-P ridge, which is rather pronounced at forward angles at the expected velocity of $4V$. A closer inspection at backward angles also shows an enhancement at about $4V$ which can be associated with the P-T-P-T process.

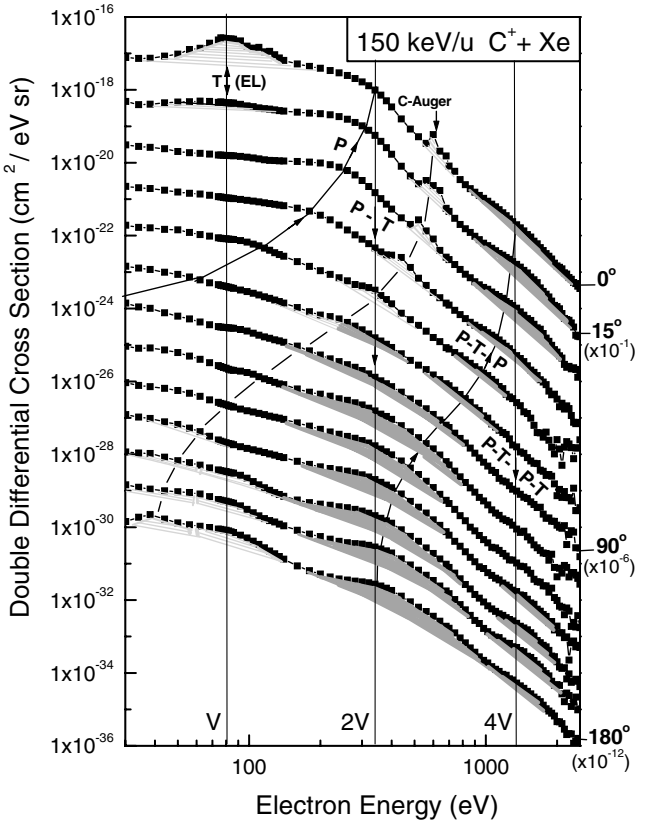

FIG. 1. Experimental double differential cross section for electron emission at 0°, 15°, . . . , 165°, 180°, in 150 keV/u C^+ + Xe collisions. Lines with arrows indicate the expected location of the T, P, P-T, P-T-P, and P-T-P-T ridges. The arrows represent the "direction of acceleration." Dominant single scattering target ionization yields (including the P process) are not shaded. Proposed multiple scattering contributions are marked by dark gray, while the C K-Auger and T components by light gray shading. Note the multiplication factors for the angular channels at the right-hand side.

The mean velocity given by Eq. (1) corresponds to a start with a target electron initially "at rest." Since backscattering needs a finite time, the length of possible sequences is limited for such electrons. Therefore, the high-momentum tail of the initial state distribution (Compton profile) could be favored, and a shift of the observed mean velocity to higher values can be expected for longer sequences. In Fig. 1, such a shift can be seen for the proposed P-T and P-T-P-T components at backward angles. This is just the opposite case from the decrease of peak energies in the first scattering due to finite binding energies (e.g., for the 0° BE peak [24]). In Fig. 1, multiple scattering processes starting with electron loss (T) might also be present. The broadening of the P-T shoulder towards higher energy at 180° may be partially associated with the T-P-T process. We note, that the T-P structure should be close to the C K-Auger group at all angles, thus decreasing the chance to observe it.

To identify the signatures of multiple scattering, one should separate them from the single scattering contributions. In order to estimate the latter components, we measured reference spectra with He^+ projectiles, where much less P-T-P contribution was expected than for C^+ impact (the calculated $\sigma_{P\text{-}T\text{-}P}/\sigma_P$ ratio was 11 times larger for C^+ than for He^+). We also performed auxiliary 1st-Born calculations for the ionization of all Xe subshells with both projectiles, according to Ref. [25].

Experiments and target ionization calculations are compared in Fig. 2, at a 15° observation angle. Good agreement has been found for the 233 keV/u He^+ projectile at electron energies above the BE peak (500 eV). Even the calculated subshell effects are observed in the experimental data in Fig. 2. We note that above 600 eV the continuous spectra are dominated by target ionization, and the 1st-Born calculations simply scale with Z^2_{proj}. Electron loss contributions and screening effects gain importance only at and below the BE peak.

Hence, instead of using the measured He^+ spectra as a direct reference, we use the 1st-Born data to represent the single scattering target ionization. This also works well for C^+ impact, where only two deviations from the 1st-Born curves are observed above 600 eV, namely, the carbon K-Auger group, and a broader structure around $4V$ for both impact velocities. These latter shoulders are attributed to the P-T-P process in C^+ + Xe collisions.

It is seen in Figs. 1 and 2, that the cross sections vary with electron energy by several orders of magnitude, whereas multiple scattering increases the yields only by a factor of 2–4. Hence, to observe the multiple scattering contributions, we remove the strong energy variations by displaying the ratio of the experimental cross sections and the 1st-Born results for the target. For the 150 keV/u C^+ + Xe collision system, this ratio is shown in Fig. 3. The energy and angular coordinates of Fig. 1 have been transformed to electron velocity components parallel (v_z) and perpendicular (v_x) to the beam direction (similar to Refs. [1,2,21]), and both v components have been divided by the projectile velocity V. In this normalized velocity space, an elastic scattering by the target and the projectile center is represented by a circle centered at the $t(0,0)$ and the $p(1,0)$ points, respectively.

The T process in Fig. 3 is strong at forward (1,0) and rather weak at backward $(-1,0)$ directions. The C K-Auger electrons show up as a circle centered at p. The P process shows only a moderate enhancement at forward angles. This deviation from the 1st-Born results is due to the non-Coulomb projectile field [18,19]. The P-T process is clearly observable at backward angles. The most significant structure in Fig. 3 is the circular P-T-P ridge centered at p, with an intense forward component at $v_z = 4V$. Finally, the P-T-P-T peak is also clearly identifiable at backward angles, at $v_z = -4V$. In summary, the contour plot provides clear evidence for double, triple, and quadruple scattering of the target electrons. The corresponding plot for the faster (233 keV/u) C^+ ion (not shown) gives an entirely similar pattern. We note that, in accordance with our free electron elastic scattering calculations, the "last" scatterings by the Xe ion (T, P-T, P-T-P-T) produce visible peaks only at about 180°, while the P-T-P process forms a circular ridge.

The plot in Fig. 3 is rich in details. For a more concise presentation, we integrated both experiment and 1st-Born theory over forward (0°–60°) and backward (120°–180°) observation angles. The ratios of the integrated cross sections are shown in Fig. 4. Distinct broad peaks appear at $2V$ in backward angles and at close to $4V$ in both forward

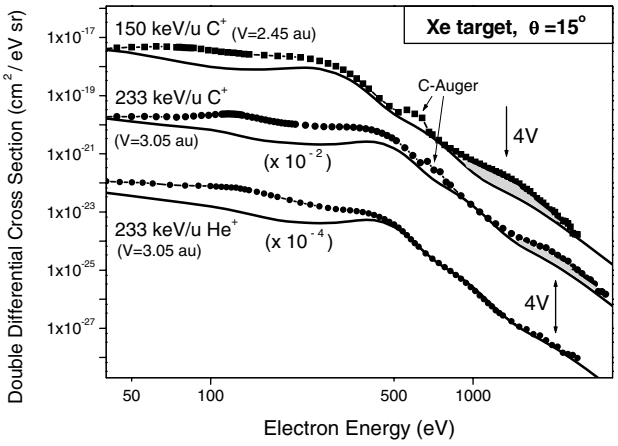

FIG. 2. Comparison between experiment and 1st-Born theory for 2.45 a.u. impact velocity C^+, and 3.05 a.u. He^+ and C^+ projectiles at 15° observation angle ($v_{P\text{-}T\text{-}P}(15°) = 3.99V \approx 4V$). Symbols: experiment; lines: target ionization theory. Note the good agreement for He^+ impact above 500 eV.

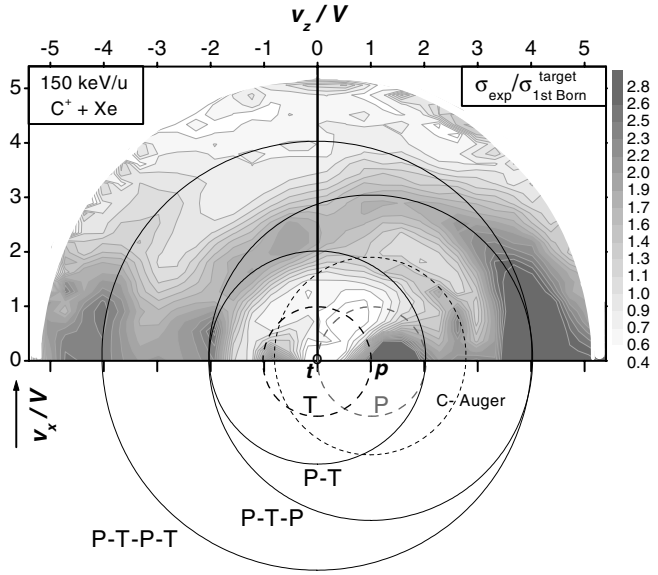

FIG. 3. Contour plot for the ratio of experiment and 1st-Born target ionization theory for 150 keV/u C^+ + Xe collisions. The normalized electron velocity components v_z/V and v_x/V are parallel and perpendicular to the beam direction, respectively.

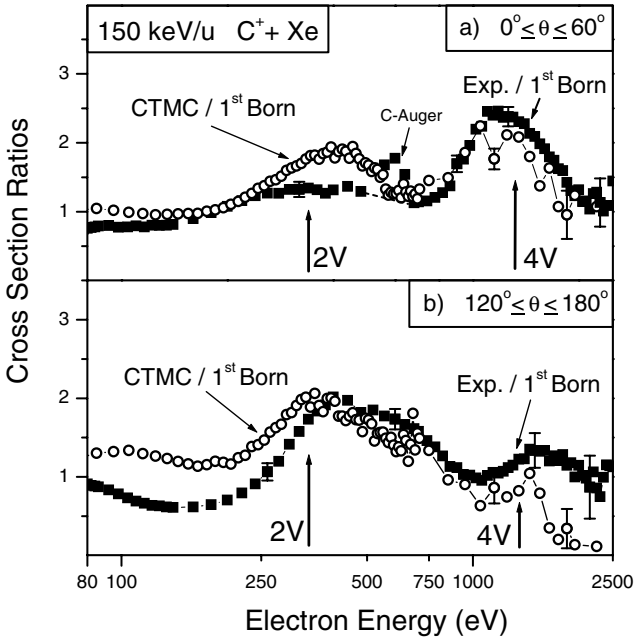

FIG. 4. Comparison between experiment and CTMC calculations. Both data sets are divided by the 1st-Born target results, and integrated over forward (a) and backward (b) observation angles. Some typical error bars are also indicated.

and backward angles. It is noteworthy to give the approximate ratios of the integrated experimental cross sections belonging to the peaks in Fig. 4. The relative *P-T*: *P-T-P*: *P-T-P-T* yields are 10 000:280:16 for 150 keV/u, and 10 000:140:6 for 233 keV/u C^+ impact. The large fractions backscattered by the xenon core in the fourth scattering ($\sim$6% for 150 and $\sim$4% for 233 keV/u) might be considered as an indication of a trapping mechanism [13].

Figure 4 also shows the results of classical trajectory Monte Carlo (CTMC) calculations [26], performed for all shells of the C^+ ion (electron loss), and for the $4d$, $5s$, and $5p$ subshells of Xe, using analytic screening potentials [27] at both collision partners. It is clearly seen that experiment and CTMC calculations provide very similar peak structures. Moreover, an analysis of the associated recoil ion momenta shows that at least 97% of the "CTMC electrons" in the peaks at $4V$ are emitted in *P-T-P* processes at forward observation angles and in *P-T-P-T* processes at backward observation angles. These results provide an independent confirmation that the experimental peaks at about $4V$ also originate from the indicated processes.

In conclusion, evidence for multiple electron scattering sequences between the projectile and the target has been found in single ion-atom collisions. We have observed triple and quadruple scattering of the electrons ejected in intermediate velocity collisions of C^+ ions with Xe atoms. In the electron spectra, we have separated and identified structures, which belong to a target ionization process involving a sequence of triple electron scattering by the projectile, the target, and the projectile core again. A ridge for quadruple scattering, corresponding to an additional encounter with the target core, has also been identified. Evidence for the above processes has been supported with the help of reference measurements using He^+ impact, and different calculations.

We are indebted to Raul O. Barrachina, Jean-Yves Chesnel, László Gulyás, Sándor Ricz, László Sarkadi, Nikolaus Stolterfoht, Sergio Suárez, John A. Tanis, and Theo J. M. Zouros for valuable discussions or comments. We acknowledge support from the Hungarian OTKA (T032942, M27839, in part T032306) and the Austrian AFFwF (P12470-TPH) grants.

[1] S. Suárez, R. O. Barrachina, and W. Meckbach, Phys. Rev. Lett. **77**, 474 (1996).
[2] U. Bechthold *et al.,* Phys. Rev. Lett. **79**, 2034 (1997).
[3] B. Sulik *et al.,* Nucl. Instrum. Methods Phys. Res., Sect. B **154**, 281 (1999); Phys. Scr. **T80**, 338 (1999).
[4] R. A. Baragiola *et al.,* Phys. Rev. A **45**, 5286 (1992).
[5] D. Schneider, G. Schiwietz, and D. DeWitt, Phys. Rev. A **47**, 3945 (1993).
[6] Y. Yamazaki *et al.,* RIKEN Accel. Prog. Rep. **24**, 54 (1990); **26**, 66 (1992); **27**, 60 (1993).
[7] H. Rothard, Nucl. Instrum. Methods Phys. Res., Sect. B **146**, 1 (1998); H. Rothard, D. H. Jakubassa-Amundsen, and A. Billebaud, J. Phys. B **31**, 1563 (1998).
[8] G. Lanzano *et al.,* Phys. Rev. Lett. **83**, 4518 (1999).
[9] E. Fermi, Phys. Rev. **75**, 1169 (1949).
[10] R. J. Beuhler, G. Friedlander, and L. Friedman, Phys. Rev. Lett. **63**, 1292 (1989).
[11] J. Burgdörfer, J. Wang, and R. H. Ritchie, Phys. Scr. **44**, 391 (1991).
[12] J. Wang, J. Burgdörfer, and A. Bárány, Phys. Rev. A **43**, 4036 (1991).
[13] Mario M. Jakas, Phys. Rev. A **52**, 866 (1995); Nucl. Instrum. Methods Phys. Res., Sect. B **115**, 255 (1996).
[14] C. O. Reinhold *et al.,* Phys. Rev. A **58**, 2611 (1998).
[15] D. H. Lee *et al.,* Phys. Rev. A **41**, 4816 (1990).
[16] N. Stolterfoht, R. D. DuBois, and R. D. Rivarola, *Electron Emission in Heavy Ion-Atom Collisions* (Springer, Berlin, 1997).
[17] S. Yu. Ovchinnikov and J. H. Macek, Nucl. Instrum. Methods Phys. Res., Sect. B **154**, 41 (1999).
[18] P. Richard *et al.,* J. Phys. B **23**, L213 (1990).
[19] T. J. M. Zouros *et al.,* Phys. Rev. A **53**, 2272 (1996).
[20] N. Stolterfoht and D. Schneider, IEEE Trans. Nucl. Sci. **26**, 1130 (1979).
[21] C. O. Reinhold and J. Burgdörfer, Phys. Rev. A **55**, 450 (1997).
[22] D. Varga *et al.,* Nucl. Instrum. Methods Phys. Res., Sect. A **313**, 163 (1992).
[23] M. E. Rudd, L. H. Toburen, and N. Stolterfoht, At. Data Nucl. Data Tables **23**, 405 (1979).
[24] H. I. Hidmi *et al.,* Phys. Rev. A **48**, 4421 (1993).
[25] R. D. DuBois and S. T. Manson, Phys. Rev. A **42**, 1222 (1990).
[26] R. E. Olson and A. Salop, Phys. Rev. A **16**, 531 (1977).
[27] R. H. Garvey *et al.,* Phys. Rev. A **12**, 1144 (1975).